Eurographics/ IEEE-VGTC Symposium on Visualization (2006)
Thomas Ertl, Ken Joy, and Beatriz Santos (Editors)

Integrated Visualization of Morphologic and Perfusion Data for the Analysis of Coronary Artery Disease

S. Oeltze[1], A. Kuß[1], F. Grothues[2], A. Hennemuth[3] and B. Preim[1]

[1]Department of Simulation and Graphics, OvG University Magdeburg, Germany
[2]Department of Cardiology, Angiology and Pneumology, OvG University Magdeburg, Germany
[3]MeVis - Center for Medical Diagnostic Systems and Visualization gGmbH, University of Bremen, Germany

Abstract

We present static and dynamic techniques to visualize perfusion data and to relate perfusion data to morphologic image data. In particular, we describe the integrated analysis of MRI myocardial perfusion data with CT coronary angiographies depicting the morphology. We refined the Bull's-Eye Plot, a wide-spread and accepted analysis tool in cardiac diagnosis, to show aggregated information of perfusion data at rest and under stress. The correlation between regions of the myocard with reduced perfusion and 3d renditions of the coronary vessels can be explored within a synchronized visualization of both. With our research, we attempt to improve the diagnosis of early stage coronary artery disease.

Categories and Subject Descriptors (according to ACM CCS): J.3 [Life and Medical Sciences]: Health

1. Introduction

The consequences of the Coronary Artery Disease (CAD) head the list of causes of death in industrial countries. Angina pectoris, cardiac arrhythmia and heart attack result from the restricted blood supply of the myocardium. At an early stage, the CAD is characterized by a perfusion defect caused by stenosis (an abnormal vessel narrowing). The localization of the perfusion defect with respect to the myocardium combined with anatomical knowledge about the supplying coronary arteries is essential in detecting stenosis as well as in early CAD diagnosis. For perfusion diagnosis, perfusion data are acquired to examine the distribution of a very fast injected contrast agent (CA) bolus over time. The data acquisition is typically accomplished according to the standards of the American Heart Association (AHA) [CWDea02] in 3-4 cardiac short axis planes. Hence, the myocardium appears ring-shaped in the images (Fig. 1). For perfusion analysis, the myocardium is then segmented and divided into 17 regions based on a correspondence between those regions and the supplying coronary branch: left circumflex (RCX), left anterior descending (LAD) and right coronary artery (RCA). The dynamic parameters characterizing the CA distribution for each region are computed, averaged and visualized separately by means of polar coordinates in a color-coded Bull's-Eye Plot (Fig. 2). In discussions between computer scientists and cardiologists it turned out that the diagnosis often requires an examination of more than a single parameter. This is also known from other application areas of perfusion imaging, such as tumor perfusion and stroke diagnosis. State of the art analysis tools only present separate single color-coded parameter visualizations which have to be integrated mentally. Hence, we study the problem of integrating several parameters in a multiparameter visualization. We extend the idea of color-coding parameter values by applying additional visualization attributes such as surface height and texture and the concept of flexible lenses. Such visualizations may improve the detection of regions exhibiting delayed and reduced perfusion.

The acquisition of perfusion data is often carried out at rest and under drug-induced stress since the stress test may reveal even marginal stenosis which are not visible at the resting state. To account for the familiarity of cardiologists with the Bull's-Eye Plot, we facilitate a comparison between the states by refining the plot.

If a suspicious region is detected in the perfusion data, the supplying coronaries may be systematically examined for the occurrence of hemodynamically relevant stenosis. Computer Tomography Coronary Angiography (CTCA) data are acquired to represent the anatomy of the coronary arteries

and the left ventricle. An integrated visualization of morphologic and perfusion data facilitates the interpretation of the perfusion study with regard to the coronary territory.

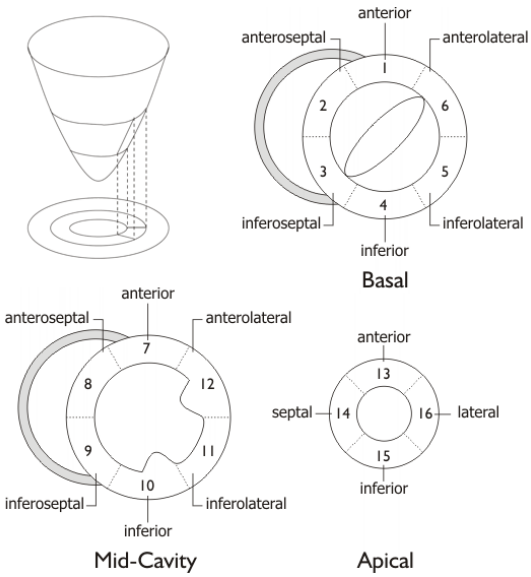

Figure 1: *AHA-conform acquisition and segmentation of myocardial perfusion data in short-axis views. Upper left: Schematic representation of the left ventricle. Typically, 3 to 4 slices are planned dissecting the left ventricle basally, centrically, apically and at the apex itself. Upper right and lower row: Nomenclature of radially distributed segments in each slice. Segment 17 is the apex itself. The right ventricle is indicated as filled semi-circle.*

In our work, we address the challenge of visually analyzing perfusion data and related datasets to improve cardiac diagnosis. Some aspects of our work are more general and relate to the exploration of perfusion data and the integrated analysis of perfusion and morphologic image data in other application areas.

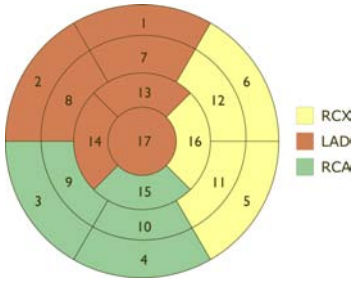

Figure 2: *Bull's-Eye Plot and AHA-conform nomenclature. The plot is generated by projecting the myocardial segments onto a plane (see Fig. 1, (upper left)). The segments are colored according to the supplying coronary branch.*

2. Medical Background

The human heart works as a pump sending oxygen-rich blood through all parts of the body. The pump mechanism is based on a regular and continuous process of contraction and relaxation of the myocardium establishing a blood circuit. Since the myocardium has a high demand on oxygen and nutrients which are delivered through the blood, a sufficient perfusion is a requirement for the functional efficiency of the heart.

2.1. Coronary Artery Disease

The blood supply of the myocardium is provided by the left and right coronary artery, which both origin from the aorta and annularly surround the heart through several branchings. A severe stenosis or occlusion of one or more coronary arteries is referred to as Coronary Artery Disease. The CAD of a certain degree causes a perfusion defect of the myocardium restricting its pump function.

The underlying cause of CAD is atherosclerosis of the coronaries. Fats and cell debris form plaques in the vessel wall that may become calcified in the further course. The so-called atherosclerotic plaque reduces the vessel diameter (stenosis) and hampers the elasticity of the vessels. A sufficient elasticity is crucial under stress conditions to account for the hearts increased demand on oxygen by vessel dilation. The gold standard for the diagnosis of coronary anatomy and atherosclerosis is conventional invasive X-ray angiography which facilitates interventional procedures albeit a certain amount of risk. The recently introduced 64-slice CT technology presents an alternative non-invasive technique. It provides a fast visualization of coronary anatomy and in clinical studies a good sensitivity and specificity in the detection of coronary artery stenosis [MCvMea05].

The response of the myocardium to ischemia occurs in a determined order referred to as ischemic cascade. The cascade starts with a diminished perfusion in the affected myocardium which results in a hampered diastolic relaxation process and subsequent decrease of systolic contractility measured by reduced myocardial thickening and inward motion. It is then that the patient experiences chest discomfort known as angina pectoris. When the blood supply of the myocardium is massively hampered or entirely absent for a period of 20 to 30 minutes, myocardial tissue is irreversibly damaged and eventually an infarct occurs.

Since the reduced myocardial perfusion represents the beginning of the ischemic cascade, a measurement of perfusion is required for early detection of coronary stenosis. Perfusion diagnostics hence supports therapy planning and monitoring e.g. for bypass surgery and percutaneous catheter revascularization, both of them restoring the flow of oxygen and nutrients to the heart.

2.2. Perfusion Diagnosis

MR perfusion diagnosis is based on the analysis of temporal signal intensity changes in image data induced by CA wash-in. In these studies, a bolus of CA is injected very fast and its distribution is imaged by a repeated acquisition of subsequent slices covering the volume of interest. The CA provides signal changes in the acquired 4d-data (3d + time) and works as a tracer of the blood. In case of a perfusion defect, the corresponding region exhibits an abnormal change in signal intensities. The spatial resolution and quality of dynamic data are often worse than those of static data and dependent on the desired temporal resolution.

Through signal intensity changes, perfusion data characterize the wash-in and wash-out behavior of a CA in interesting tissue. By means of plotting signal intensities of corresponding voxels over time, time-intensity curves are generated. Typical dynamic parameters that characterize the perfusion of the tissue are (see Fig. 3):

- baseline. Average of signal intensities before CA arrival.
- peak enhancement (PE). The maximum intensity (over all time points).
- time to peak (TTP). The time period between the beginning of CA arrival and PE. This parameter allows to assess whether blood supply is delayed in a particular region.
- up-slope. slope between beginning of CA arrival and PE.
- integral. For a certain range of time (often representing one cycle of blood flow) the area between the curve and the baseline is computed. The parameters PE and integral together give a hint on reduced blood flow.
- mean transit time (MTT). In the range of times used for the integral calculation, MTT specifies the time t where the area left and right from t are the same. The MTT is a measure for the symmetry of the curve.

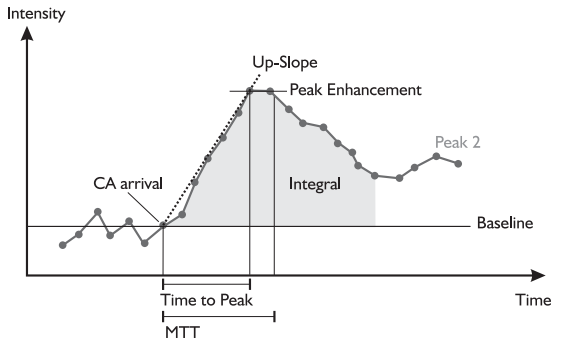

Figure 3: *Schematic representation of a typical time-intensity curve and labeling of characteristic dynamic parameters. The first pass of the CA causes the highest intensity changes and is therefore utilized for parameter derivation. Subsequent passes (Peak 2) are not considered normally.*

2.3. Myocardial Perfusion Diagnosis

The prevailing imaging technique in cardiac perfusion diagnosis is nuclear imaging, in particular SPECT and positron emission tomography (PET), more recently tackled by advances in ultrasound and MRI. The latter is pioneering and gaining in importance since it has shown at least a similar sensitivity and specificity in comparison to SPECT while providing a higher spatial resolution [SNKea01].

The data acquisition in cardiac perfusion imaging is typically accomplished AHA-conform [CWDea02] in 3-4 cardiac short axis planes. The slices are acquired during breath-hold and electrocardiogram (ECG)-triggered over a period of at least 40 consecutive heart beats. Typical dataset dimensions are $128 \times 128 \times (3-4) \times 40$ with an in-plane resolution of $\approx 1.5 \times 1.5mm$ and a slice thickness of $7-8mm$. The acquisition of perfusion data is often carried out at rest and under drug-induced stress. At rest, the autoregulation of the heart may compensate the restricted blood flow due to stenosis resulting in no significant signal intensity changes. The stress test may reveal even marginal stenosis and is usually performed prior to the test at rest using identical imaging parameters. Altogether, during the examination up to 320 images are generated requiring dedicated exploration and analysis tools to support the diagnosis.

An initial overview of the data is often conducted visually in cine-mode. However, this examination is subjective and hence user-dependent, it does not deliver quantitative results, small perfusion defects may remain undetected and the comparison of rest and stress data requires a mental integration of suspicious regions. Therefore, the visual inspection should ideally be followed by a semi-quantitative analysis of the time-intensity curves that is to say the computation of dynamic parameters that characterize the perfusion (recall Sec.2.2). For myocardial perfusion diagnosis, the parameters PE, TTP, up-slope and MTT have been evaluated as especially meaningful. In [ASNGea00], the up-slope is validated as the most sensitive parameter for the detection of myocardial ischemia. Based on the ratio of the up-slope at rest and under stress, a so-called myocardial perfusion reserve index (MPRI) may be computed. The coronary perfusion reserve is defined as the ability of the coronary arteries to increase blood flow under stress by a factor of up to 4-5 by vessel dilation in comparison to the resting state. The MPRI facilitates a more reliable detection of ischemic areas. A MPRI value of 1.5 was found to be the threshold between ischemic and non-ischemic tissue [ASNGea00].

3. Prior and Related Work

Commercial workstations [Sie05] and software packages [Imp05], [Med05] by default allow the definition of Regions of Interest (ROI), a semi-quantitative analysis of the corresponding averaged time-intensity curves and a visualization of the calculated parameters by means of polar coordinates

in a Bull's-Eye Plot (Fig. 2). The latter is constructed according to suggestions of the AHA [CWDea02]. The myocardium is divided into 17 segments, parameters are averaged and color-coded for each segment. Due to the rough division, the precise extension of an ischemic region remains uncertain. Hence, some analysis tools permit a more subtle division. In [PGYea01], a pixel-wise examination using color-coded parameter maps is suggested. This technique has early been assessed as useful in the context of kidney perfusion by [HOB81]. Quantitative analysis of the blood flow using MRI is merely possible with the help of highly complex, not yet evaluated models.

In other application areas of perfusion imaging, the computation of subtraction images between two points of time was presented [MMSJea99]. Such images reveal differences in signal intensity indicating contrast enhancement. Despite being a simple approach, the definition of two points of time providing a meaningful subtraction image is complicated in the context of the examined Dynamic Contrast Enhanced MR-mammographies (DCE_MRM). DCE_MRM with a relatively high spatial resolution (> 50 slices) lend themselves for volume rendering [CGBea05]. By means of interactively mapping dynamic parameters to transparency and rotating the object, an examination of tumors in the female breast is facilitated. A color-coded Closest Vessel Projection especially suitable for visualizing parameters derived from DCE_MRM was presented in [KPWea02].

Integration of Morphologic and Perfusion Data

Many studies [ASGBea01], [GNCea04] exploit the correspondence between myocardial perfusion and the supplying coronary arteries for CAD detection using the 17 segment model (see above) with assumed coronary artery distribution [CWDea02]. Since only $\approx 80\%$ of the patients match this distribution, in [SJAea03] an approach was suggested that validates whether a patient complies to the model by comparing the predefined coronary territory assignment with the actual angiographically derived coronary distribution. As the results indicate, the combination of image information for each individual improves diagnostic accuracy. The 3d-fusion of single photon emission computed tomography (SPECT) perfusion data and X-ray coronary angiography (CAG) data is presented in [SMJea99]. The coronary tree is reconstructed from biplane projections and the left ventricular surface is extracted from interpolated SPECT data. The 3d-representation of the coronaries together with a mapping of the perfusion data to the ventricle allow an accurate assignment of particular myocardial perfusion regions to the corresponding vessels. Since the reconstruction of the coronaries from CAG data induces spatial distortion and CAG is an expensive and invasive procedure, [NKCea05] studied the fusion of CTCA and SPECT. After the coronary arteries and the left ventricle are segmented and visualized in 3d, the SPECT data are mapped to the ventricle.

4. Multiparameter Visualization for Myocardial Perfusion Diagnosis

To account for the drawbacks of isolated single parameter visualizations, we present multiparameter visualization techniques for the integrated representation of dynamic parameters.

4.1. Preprocessing of the Perfusion Data

For perfusion diagnosis, the parameters introduced in Sec. 2.2 are derived per voxel and stored in separate parameter volumes. These volumes are computed for the rest and the stress state based on the respective perfusion data. As a preprocessing step, the perfusion data is motion-corrected to establish a valid inter-pixel correspondence. We used a combination of rigid and elastic registration employing mutual information as the similarity measure and a gradient descent method for optimization purposes [RSHea99]. For parameter computation, the user applies the motion-corrected perfusion data set and selects a ROI in healthy myocardial tissue. Based on the time-intensity curve of this ROI, the user manually determines characteristic curve points such as the time of CA arrival, PE and the end of the first pass. Utilizing these points, the parameters are calculated for each voxel of the data set by means of simple mathematics.

4.2. Refined Bull's-Eye Plot for Rest/Stress Comparison

In a rest/stress comparison, (multi)parameter visualizations may be displayed side by side to identify areas where either perfusion defects first appear under stress or resting defects become worse with stress. We simplify a mental integration of rest and stress perfusion in one area by opposing one parameter of both states in a single visualization. To account for the familiarity of cardiologists with the Bull's-Eye Plot, we first refined the plot. Each segment ring is bisected thus duplicating the number of segments. The resulting outer and inner rings represent the stress and the rest state, respectively (Fig. 4). This circular bisection instead of a radial bisection ensures that neighboring segments in the plot are adjacent in the myocardium as well and show the same state. The refined plot may be used for comparing two different parameters of one state as well.

4.3. Colored Heightfields

Colored heightfields enable the integrated visualization of two parameter maps. A 3d-elevation profile is generated based on the pixel-values of the first parameter map. In a next step, the resulting profile is colored according to the pixel-values of the second parameter map and an arbitrary color look-up-table (Fig. 5). The profile may be freely rotated such that initially occluded parts become visible. The mapping to height is scalable. It is initially adapted to the domain of the first parameter. A local illumination simplifies

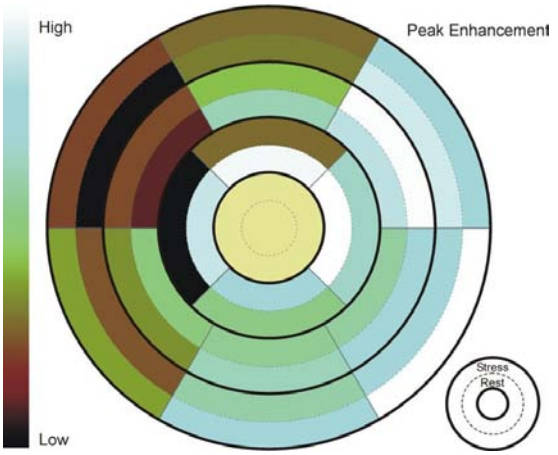

Figure 4: *Integrated visualization of the parameter PE for the rest and stress state in a refined Bull's-Eye Plot. An ischemic area is revealed in each slice (ring) from anterior to inferoseptal along the septum. Dark regions mark a diminished perfusion. Apically the perfusion defect may remain unnoticed if perfusion is only examined at rest. Segment 17 is missing since no slice has been acquired at the apex itself.*

the detection of small differences in height. The isometric projection and a linear interpolation of the parameter values guarantee the non-ambiguous relation between visualization and underlying data. Distinctive heights, e.g. strong maxima, are labeled. In addition, a grid may be overlaid on the profile. The resulting curvature of the lines illustrates homogeneity and inhomogeneity, respectively.

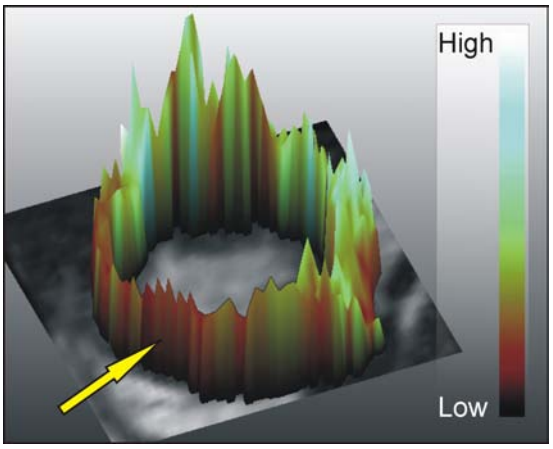

Figure 5: *Colored heightfield based on parameters PE (height) and up-slope (color). Small elevations (diminished perfusion) and dark colors (delayed perfusion) represent ischemic territories. The corresponding original slice at an adjustable time-point serves as context information.*

4.4. Flexible Synchronized Lenses

Lenses are often applied in exploring medical image data for the magnification of small suspicious details. They may be utilized as well for the integration of additional information in multiparameter visualizations. Relating to parameter maps, one parameter may be displayed within the lens (focus) in the context of another parameter or the original slice. For that purpose, an axis-aligned, relocatable and resizable lens is positioned by the user, e.g. on a parameter map. Next, the second parameter map is projected through the lens onto the first map. Both maps are color-coded each with an arbitrary color look-up-table (Fig. 6).

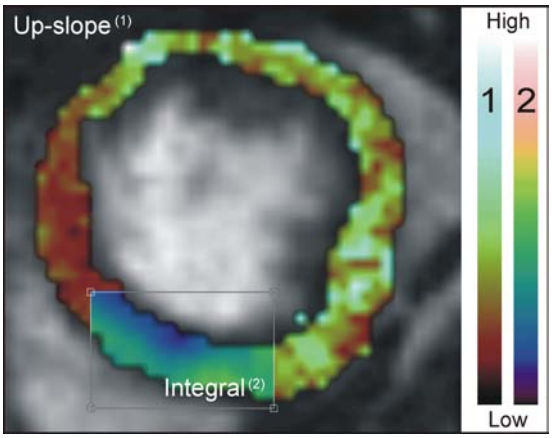

Figure 6: *Parameter up-slope is displayed for the myocardium in the context of an original slice. Parameter integral is projected through a user-defined lens. Dark inferior and septal regions indicate a perfusion defect.*

In cerebral perfusion diagnosis, synchronized lenses exploit the symmetry of the brain in axial views. A lens is mirrored on a relocatable, vertical line of symmetry to detect differences between both hemispheres.

4.5. Color Icons

By means of color icons several parameter maps can be integrated into one visualization. Since the integration of > 4 parameters is clinically not relevant, we replace each pixel of the original slice by four new, quadratically arranged pixels (color icon). A mapping to an arbitrary color is defined for each pixel of the icon and the intensities of the corresponding pixels in up to four parameter maps are then assigned to the newly generated pixels (Fig. 7). The perception of the resulting texture conveys the global distribution of certain parameter combinations. The user may zoom in on an interesting structure for better recognition of the underlying texture. The application of color icons is inspired by [Lev91].

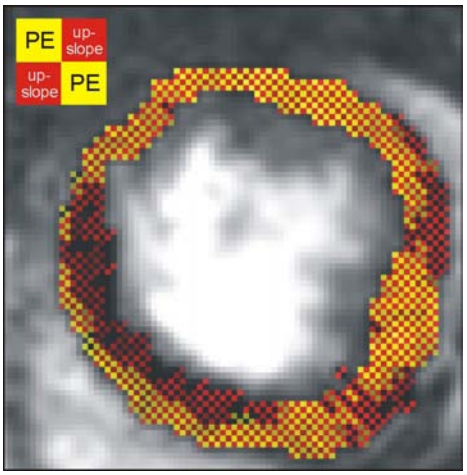

Figure 7: *Color icons illustrating the parameters PE and up-slope. The icon's structure is represented as an inlet. Septal, a large dark area is characterized by diminished and delayed perfusion indicating a serious perfusion defect. Inferolateral, slight perfusion disturbances are observed.*

5. Integrated Visualization of Morphologic and Perfusion Data

The detection of myocardial regions exhibiting delayed and decreased perfusion by means of multiparameter visualizations may be followed by an examination of the supplying coronary arteries. For this purpose, we apply an integrated visualization of the perfusion analysis results and the morphologic data from CTCA images, in particular the coronaries, the epicardial left ventricle and the aorta ascendens. We establish a bidirectional link between the Bull's-Eye Plot representing perfusion analysis results and a 3d-view showing the coronaries, the ventricle and the aorta.

5.1. Preprocessing of the Morphologic Data

In a first step, the epicardial left ventricle is segmented from the CTCA data using live-wire as an edge-based segmentation method [SPP00]. Hereby, the live-wire algorithm is applied on individually user-selected slices. Intermediate contours are computed utilizing shape-based interpolation and optimized according to the live-wire cost function. As a preprocessing step, the resulting binary ventricle mask is resampled and then smoothed by a Gaussian kernel to enhance the quality of the epicardial surface extracted by a threshold-based 3d-surface visualization. Accuracy is not a critical issue here since the ventricle only serves as context information. In a next step, the coronary tree is segmented from the original CTCA data (no preprocessing) by means of an advanced 3d region growing algorithm [HBBea05]. The aorta ascendens is manually separated from the vessel segmentation result, stored in an extra data set and preprocessed and visualized similar to the left ventricle. For the remaining coronary arteries, the vessel skeleton and associated radius information is then extracted with the help of a thinning algorithm presented in [SPSea02]. The three main branches of the coronaries, RCX, LAD and RCA, are identified manually according to the ventricular territory they supply and assigned a unique color. The skeleton as well as the coloring serve as an input for the visualization of the coronaries by means of Convolution Surfaces [OP05]. Polygonal models of the left ventricle, the aorta ascendens and the coronary arteries are eventually combined in a single 3d-view.

5.2. Interactive Bull's-Eye Plot

The link between the Bull's-Eye Plot and the 3d-view, in particular the coronaries, is established by assigning a unique *ID* to the polygonal models of the three main branches. The same *ID* is assigned to each segment of the plot which is supplied by the respective branch according to the standardized correspondence [CWDea02]. Furthermore, picking facilities are implemented for both, the plot and the 3d-view. A segment of the plot exhibiting a suspicious parameter value may now be selected by the user via mouse interaction. The previously assigned *ID* is retrieved and the corresponding vessel branch is focussed in the 3d-view (Fig. 8).

Focussing of objects benefits from animations since the user is guided through the scene instead of being confronted only with the interaction results. For focussing purposes, we apply animation scripts based on a script language independent of the underlying data [MBP06]. The script language allows to define appropriate points of view for each object of interest which serve as an input for computing animations in-between.

To focus the coronary branches, the animation script requires a predefined appropriate view-point for each branch. This definition is accomplished by the user so far. However, the process is supported based on computing a sphere S enclosing the entire scene. As the center c of S, we determine the center of the scene's bounding box BB. To include the whole scene, the radius r of S is computed as the distance between the furthermost vertex of BB and c. Next, the viewpoint is determined manually for each branch by moving the camera along a trajectory on S. The camera position is modified via the script language by applying the trigonometric description of a sphere and varying azimuth and elevation angle. Zooming in and out is supported as well. Once ideal view-points were determined, the corresponding angle values and zooming factors are stored in a separate file for each branch. When the user selects a segment in the Bull's-Eye Plot, the corresponding file is fed into the script interpreter. The interpreter then performs the animated motion from the current camera position to the stored ideal view-point and lets the camera orbit the ventricle.

As mentioned earlier in this section, the link between

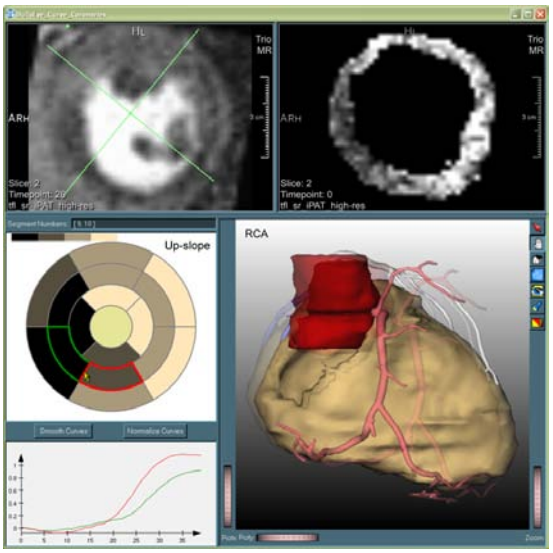

Figure 8: *Anatomy and myocardial perfusion of a patient suffering from atherosclerosis of the RCA and the LAD. Upper left: Apical slice of the original perfusion data set and the AHA-consistent segmentation of the myocardium overlaid. Upper right: Apical slice of the parameter volume computed for up-slope. Middle left: Selection of 2 segments in the Bull's-Eye Plot which color-codes the parameter up-slope. Segment 17 is missing since no slice has been acquired at the apex itself. Lower left: Time-intensity curves corresponding to the selected segments. Lower Right: Coronary branch (RCA) supplying the selected segments. The animated focussing is illustrated by a semitransparent overlay of a previous point in time.*

the Bull's-Eye Plot and the 3d-view is bidirectional. The user may select a coronary branch in the 3d-view by picking via mouse interaction as well. Based on the correspondence between the coronaries and the myocardial regions they supply, the respective segments of the Bull's-Eye Plot are highlighted and the associated time-intensity curves are displayed. Regarding the 3d-view, the camera moves to the ideal view-point defined for the selected branch. For further focussing the selection, the other branches are rendered semi-transparently while the selected branch is rendered opaque (Fig. 9). In addition, the saturation of the surface colors of the left ventricle and the ascending aorta is strongly reduced. The change in material properties is animated as well over a predefined period of time.

5.3. Model-based Integration of Morphologic and Perfusion Data

Due to the high cost of CTCA, these data are rarely acquired in combination with perfusion data. Therefore, we apply standard models of the ventricle and the coronaries

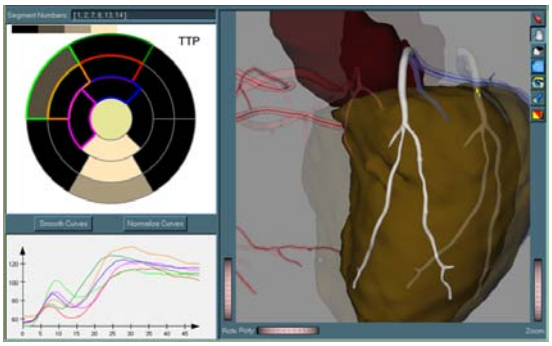

Figure 9: *Selection and focus of a coronary branch (LAD). The course of the animation is illustrated by a superimposition of a previous point in time. The other branches are rendered semi-transparent with the vessel skeleton overlaid to enhance spatial comprehensibility. The segments of the Bull's-Eye Plot which correspond to myocardial regions supplied by the selected branch are highlighted. The respective time-intensity curves are visualized.*

derived from a healthy subject. The models allow an accentuation of suspicious vessel sections and provide a communication basis for the cardiologist and other health professionals. However, it is crucial to keep in mind that the standardized assignment of the supplying territories is only valid for $\approx 80\%$ of the population.

6. Conclusions

We presented visualization techniques for the analysis of perfusion data. In particular, the analysis of different parameters characterizing time-intensity curves for a particular voxel is supported. Colored icons, colored heightfields and flexible lenses turned out to be useful for the integrated visualization of different parameters. The visualization of perfusion parameters can be combined with the visualization of anatomic data in order to enhance the overview. For the analysis of myocardial perfusion, we support the analysis of perfusion data at rest and under stress. The Bull's-Eye Plot which is frequently used for CAD diagnosis is refined to support the rest/stress comparison of perfusion parameters. The correlation between Bull's-Eye Plot segments and the corresponding vascular structure is considered to allow a synchronized selection. The design and refinement of visualization techniques is guided by urgent diagnostic questions and informally discussed within clinical cooperations. The integration of these techniques in a usable software assistant and a more systematic evaluation is left open for future work. The latter requires representative cases for CAD or infarct diagnosis, monitoring the use of the software assistant by cardiologists as well as comparing speed and accuracy of the analysis to established commercial systems.

Acknowledgements

We want to thank the Max Planck MR-center of the University Tübingen and the Department of Radiology of the University Erlangen for providing the image data our work is based on. Furthermore, we are indebted to C. Kühnel for preparing the image analysis results based on the CTCA data and for fruitful discussions. We are grateful to K. Mühler for integrating his animation scripting system.

References

[ASGBea01] AL-SAADI N., GROSS M., BORNSTEDT A., ET AL.: Comparison of various parameters for determining an index of myocardial perfusion reserve in detecting coronary stenosis with cardiovascular magnetic resonance tomography. *Z Kardiol 90*, 11 (Nov 2001), 824–34.

[ASNGea00] AL-SAADI N., NAGEL E., GROSS M., ET AL.: Noninvasive detection of myocardial ischemia from perfusion reserve based on cardiovascular magnetic resonance. *Circulation 101*, 12 (Mar 2000), 1379–83.

[CGBea05] COTO E., GRIMM S., BRUCKNER S., ET AL.: MammoExplorer: An Advanced CAD Application for Breast DCE-MRI. In *VMV* (2005), pp. 91–98.

[CWDea02] CERQUEIRA M., WEISSMAN N., DILSIZIAN V., ET AL.: Standardized myocardial segmentation and nomenclature for tomographic imaging of the heart. *Circulation 105*, 4 (Jan 2002), 539–42.

[GNCea04] GIANG T., NANZ D., COULDEN R., ET AL.: Detection of coronary artery disease by magnetic resonance myocardial perfusion imaging with various contrast medium doses: first European multi-centre experience. *Eur Heart J 25*, 18 (Sep 2004), 1657–65.

[HBBea05] HENNEMUTH A., BOCK S., BOSKAMP T., ET AL.: One-click coronary tree segmentation in ct angiographic images. In *CARS* (2005), pp. 317–21.

[HOB81] HOEHNE K., OBERMOELLER U., BOEHM M.: X-Ray Functional Imaging - Evaluation of the Properties of Different Parameters. In *Proc. Conference on Digital Radiography* (1981), pp. 224–228.

[Imp05] IMPERIALCOLLEGE: CMRtools. http://www.cmrtools.com, Dec 2005.

[KPWea02] KOHLE S., PREIM B., WIENER J., ET AL.: Exploration of time-varying data for medical diagnosis. In *VMV* (2002), Amsterdam: IOS Press, pp. 31–8.

[Lev91] LEVKOWITZ H.: Color icons: merging color and texture perception for integrated visualization of multiple parameters. In *IEEE Visualization* (1991), pp. 164–170.

[MBP06] MÜHLER K., BADE R., PREIM B.: Skriptbasierte Animationen für die Operationsplanung und Ausbildung. In *Bildverarbeitung für die Medizin* (2006), Informatik aktuell, Springer.

[MCvMea05] MOLLET N., CADEMARTIRI F., VAN MIEGHEM C., ET AL.: High-resolution spiral computed tomography coronary angiography in patients referred for diagnostic conventional coronary angiography. *Circulation 112*, 15 (Oct 2005), 2318–23.

[Med05] MEDIS: QMassMR. http://www.medis.nl, Dec 2005.

[MMSJea99] MEYER S., MÜLLER-SCHIMPFLE M., JÜRGENS H., ET AL.: MT-DYNA: Computer assistance for the evaluation of dynamic MR and CT data in a clinical environment. In *CARS* (1999), pp. 331–334.

[NKCea05] NAKAJO H., KUMITA S., CHO K., ET AL.: Three-dimensional registration of myocardial perfusion SPECT and CT coronary angiography. *Ann Nucl Med 19*, 3 (May 2005), 207–15.

[OP05] OELTZE S., PREIM B.: Visualization of vasculature with convolution surfaces: method, validation and evaluation. *IEEE Trans Med Imaging 24*, 4 (Apr 2005), 540–8.

[PGYea01] PANTING J., GATEHOUSE P., YANG G., ET AL.: Echo-planar magnetic resonance myocardial perfusion imaging: parametric map analysis and comparison with thallium SPECT. *J Magn Reson Imaging 13*, 2 (Feb 2001), 192–200.

[RSHea99] RUECKERT D., SONODA L., HAYES C., ET AL.: Nonrigid registration using free-form deformations: application to breast MR images. *IEEE Trans Med Imaging 18*, 8 (Aug 1999), 712–21.

[Sie05] SIEMENS: Argus Dynamic Signal. http://www.siemens.de, Dec 2005.

[SJAea03] SCHWARTZ J., JOHNSON R., AEPFELBACHER F., ET AL.: Sensitivity, specificity and accuracy of stress SPECT myocardial perfusion imaging for detection of coronary artery disease. *Nucl Med Commun 24*, 5 (May 2003), 543–9.

[SMJea99] SCHINDLER T., MAGOSAKI N., JESERICH M., ET AL.: Fusion imaging: combined visualization of 3D reconstructed coronary artery tree and 3D myocardial scintigraphic image in coronary artery disease. *Int J Card Imaging 15*, 5 (Oct 1999), 357–68; discussion 369–70.

[SNKea01] SCHWITTER J., NANZ D., KNEIFEL S., ET AL.: Assessment of myocardial perfusion in coronary artery disease by magnetic resonance: a comparison with positron emission tomography and coronary angiography. *Circulation 103*, 18 (May 2001), 2230–5.

[SPP00] SCHENK A., PRAUSE G., PEITGEN H.-O.: Efficient semiautomatic segmentation of 3d objects in medical images. In *MICCAI* (2000), Springer, pp. 186–195.

[SPSea02] SELLE D., PREIM B., SCHENK A., ET AL.: Analysis of vasculature for liver surgical planning. *IEEE Trans. Med. Imag. 21*, 11 (2002), 1344–1357.